IABSE-JSCE Joint Conference on Advances in Bridge Engineering-IV, August 26-27, 2020, Dhaka, Bangladesh
Amin, Okui, Bhuiyan, Rahman (eds.)
ISBN: 978-984-34-8313-3
www.iabse-bd.org

Seismic performance of lead-rubber bearing isolated bridge under long-duration ground motion

A.L. Hassan and A.H.M.M. Billah
Lakehead University, Thunder Bay, ON, Canada

ABSTRACT: This paper compares the seismic response of a base-isolated bridge under long duration ground motions. A typical multi-span continuous concrete girder bridge equipped with conventional lead rubber bearing (LRB) and Shape memory alloy wire-based lead rubber bearing (SLRB) has been considered in this study. Using advanced nonlinear seismic isolator models, the response of the bridge is evaluated under long-duration motions and compared with spectrally equivalent short duration motions. Comparable design of the both isolation systems is achieved through ensuring similar isolation period of the bridges. Response parameters considered for this study are the base shear in the piers, the acceleration of the bridge deck, maximum and residual displacement of the isolation bearings as well as the energy dissipation capacity. The results indicate that long-duration motions cause more damage to different bridge components as compared to the short-duration motions in-terms of higher deck acceleration, pier base shear, and residual isolator displacement.

1 INTRODUCTION

One of the major objectives of structural engineers and researchers is to protect structure from devastating effects of earthquake by minimizing the structural damage and loss of lives. Among many alternatives, seismic isolation is one of the most widely used and accepted methods for reducing the seismic demand on structures and improving seismic performance. Past earthquake events around the world have demonstrated the resilience of base isolated structures against extreme earthquakes. Efficiency of seismic isolation bearings for seismic protection of structures is well recognized (Tongaonkar and Jangid 2003, Warn and Whittaker 2004, Amin et al. 2006, Alam et al. 2012). Compared to buildings, isolation bearings are the favorable choice for bridges for seismic upgrade of existing structures and new constructions.

The aim of bridge seismic isolation is to decouple the superstructure response from a seismic excitation thus reducing the deck acceleration and force transmitted to the substructure. Seismic isolation limits the load transmitted from the superstructure to the substructure by introducing significant displacement of the superstructure in extreme seismic events. An effective seismic isolation provides the bridge with adequate flexibility to shift the natural period away from the predominant earthquake period. This helps avoiding resonance which could result major damage or even collapse of the bridge.

Different types of rubber-based seismic isolation bearings such as high damping rubber bearings (HDRB), steel-reinforced elastomeric bearings (SREB), lead rubber bearings (LRB), fiber-reinforced elastomeric bearings (FREB), and friction pendulum systems (FPS) have gained popularity for effective seismic control and improving the seismic performance of infrastructures (Bhuiyan and Alam 2012, Al-Anany et al. 2018,Billah and Todorov 2019). Among different seismic isolation systems, LRBs have gained much popularity and have been implemented in numerous new construction and retrofit applications. This can be attributed to the simplicity of LRB system as well as the combined isolation, energy dissipation, and re-centering function provided as a single-compact unit (Ozdemir et al. 2011).

Over the last decade, world has experienced several major earthquakes of high magnitude that lasted for a long period of time. For instance, the approximate duration of the magnitude (Mw) 9.0 Tohoku earthquake in Japan (2011), the Mw 8.8 Chile earthquake (2010), and the Mw 7.9 Wenchuan Earthquake in China (2008) were 300, 200, and 180 seconds, respectively. Long duration (LD) motions are typically generated from two sources, long rupture length and sites with softer soils. LD motions typically occur in subduction zones which are located at plate boundaries such as Tokyo (Japan), Taipei (Taiwan), and Santiago (Chile).Recent studies

(Marafietl. 2019) reported that structures having fundamental vibration period of 1.0 second or larger is more susceptible under LD ground motions. Bridge structures equipped with isolation bearings usually possess a fundamental period of vibration longer than 1.0 seconds. As a result, identifying the performance of base-isolated bridges under LD ground motions is necessary for ensuring adequate performance under LD motions.

Many past studies evaluated the performance and efficiency of different isolation systems under wide range of ground motions while mostly focusing on near-fault and far field motions. Shen et al. (2004) evaluated the performance of a lead rubber bearing isolated bridge under pulse-like near-fault motions. They found that when the pulse period of the ground motion is close to the effective period of the system, the bridge response is amplified. Dicleli (2006) studied the impact of substructure and isolator properties along with the frequency characteristics of the ground motions on the performance of seismic isolated bridges. They identified the selection of ground motions according to the site characteristics as a major factor for effective isolation system design. Ozbulut and Hurlebaus (2011) investigated the comparative performance of different isolation bearings under near-fault motions. Eröz and Des Roches (2013) compared the performance of LRB and FPS isolation bearings in a typical Multi-Span Continuous Concrete Girder bridge considering the effect of vertical ground motion. They concluded that both FPS and LRB improved the seismic performance of the bridge comparably. Although the vast literature supports the advantages of seismic isolation, no literature can be found that investigated the seismic performance of isolated bridges under long duration motions. This study aims to evaluate the seismic response of isolated bridges under long duration motions.

Many past studies have investigated the effectiveness of shape memory alloy (SMA) in vibration control and structural damage mitigation. To overcome the limitations of different rubber-based and friction-based bearings, researchers have proposed different SMA-based bearings (Alam et al. 2012, Ozbulut and Hurlebaus2011, Dezfuli and Alam 2018). This study employed two different isolation systems and spectrally matched long and short duration record sets to demonstrate the effect of ground motion duration on the seismic response of isolated bridges. Two isolation bearings are considered in this study, such as lead rubber bearing (LRB) and Shape memory alloy wire-based lead rubber bearing (SLRB). Using 20 long-duration (LD) motions and 20 spectrally matched short duration (SD) records, the performance of a three-span bridge isolated with three different isolation systems is evaluated. Response parameters considered for this study are the base shear in the piers, the acceleration of the bridge deck, maximum and residual displacement of the isolation bearings as well as the energy dissipation capacity.

2 BRIDGE DESCRIPTION

A three-span continuous concrete girder bridge located in Victoria, British Columbia, Canada is considered in this study. The bridge superstructure is supported on two-column bents with unequal bent heights of 15.5 m and 11.5m. The concrete superstructure is composed of 250mm thick cast in place concrete slab supported on three simply supported precast concrete I-girders (NU 2000) girders at 4.5m spacing as shown in Figure 1. The existing bridge is not equipped with seismic isolation bearings. The concrete superstructure sits on elastomeric pads at each abutment and pier locations. Each column bent has two circular piers connected by a rectangular concrete pier cap. The column spacing within a bent is 6.6m. The 1500 mm circular reinforced concrete piers are reinforced with 28-30M (diameter 29.9mm) longitudinal rebars and 15M (diameter 16mm) bars as spiral reinforcement. The considered bridge is classified as a major route bridge according to the current Canadian Highway Bridge Design Code (CHBDC 2019). However, with the current structural configuration, the bridge does not satisfy the performance requirements of a major route bridge outlined in CHBDC. The bridge is founded on deep foundations both at the pier and abutment locations which consist of steel HP - Bearing Piles The pier columns sit on a rectangular concrete pile cap which is connected to two rows of steel HP Piles. Conventional seat type abutments supported on steel HP piles support the bridge ends. The details of the geometric properties of different bridge components are provided in Table 1.

Table 1. Geometries properties of the bridge

Properties	Dimension	Unit
Dimension of the pier cap (L x d x w)	11,392 x1,600 x 1,800	mm
Dimension of pier (diameter)	1500	mm
Dimension of the pier pile cap (L x d x w)	12,500 x 1,800 x 4,000	mm
Deck Thickness	250	mm
Pile Section	HP 360 x 132	
Girder Section	NU2000	
Length of pile (varies)	20-25	m
No. of piles at pier	12	
No. of piles at abutment	12	

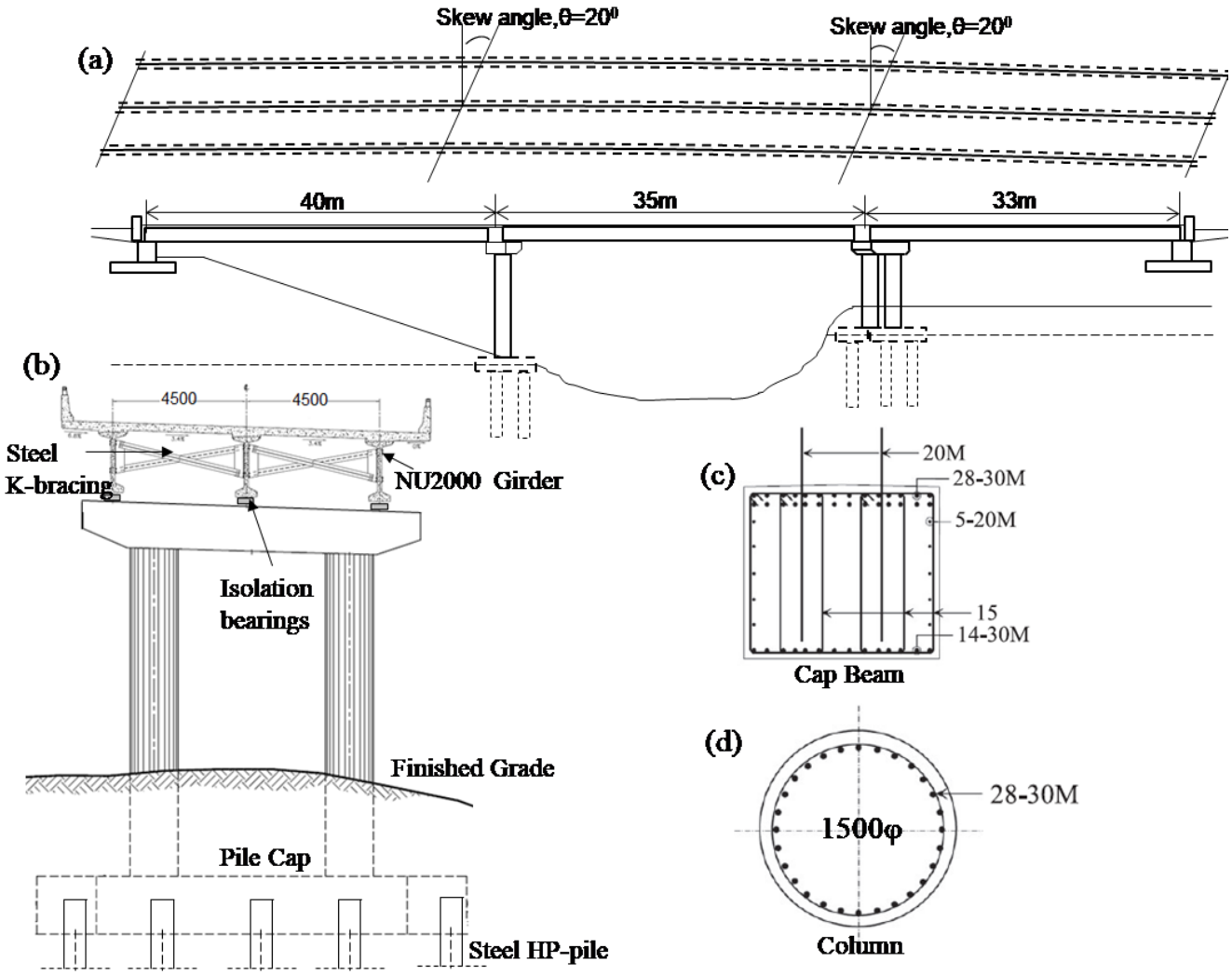

Figure 1. (a) Plan and elevation of the bridge, (b) Typical cross section at pier location, (c) Cross section of the pier cap beam, and (d) Cross section of the column.

3 SELECTION OF GROUND MOTION

Previous researchers (Chandramohan et al. 2016) suggested that spectral shapes need to be taken into account when assessing structural response to long-duration motions. While investigating the ground motion duration effect on the seismic response of structures, it is desirable to compare the response with 'similar' short duration ground motion. This "similarity" can be achieved by matching the spectral acceleration shape (Baker and Cornell 2006). In this study, the duration effect on the seismic response is evaluated by comparing the responses under a long-duration record set and a spectrally matched short-duration record set both containing 20 ground motions.

In this study, first, a set of 50 long-duration ground motions are selected from six different historical earthquake events: 2011 Tohoku, Japan; 2010 Maule, Chile; 2007 Sumatra, Indonesia; 2003 Hokkaido; Japan, 1999 Chichi, Taiwan; and 1985 Valparaiso, Chile. These ground motion records are obtained from the PEER NGA West2 ground motion database (Ancheta et al. 2011) and the Center for Engineering Strong Motion Data (CESMD 2011). The list of selected long duration motions is provided in Table 1. Among these ground motions, records having $t_{D5\text{-}75} > 25$ sec are selected as the long duration motions. All the selected ground motions have a PGA > 0.1g and PGV > 10cm/sec. This ground motion selection process provided a suite of long duration motions containing 32 records, with a geometric mean $D_{s5\text{-}75}$ of 34 sec. In order to compare the seismic performance of the three isolated bridges under long and short duration motions, another 40 ground motions are selected from the PEER NGA-West2 database. Among these ground motions, records having $D_{s5\text{-}75} <$ 20 sec and epicentral distance of more than 15km are selected. The short duration accelerograms are selected using the spectral equivalency approach of Chandramohan et al. (2016) which resulted in similar spectral shapes like the long duration counterpart in the period range of [0.05, 4.00] s. In order to minimize the sum of squared error differences of the 5%-damped linear response spectra associated with each pair of short and long duration records, a matching process is performed. To minimize the error, the short duration motions are

amplitude scaled, without affecting the frequency content of the ground motions, when necessary using a simple amplitude scaling factor of up to 5. This resulted in the creation of a spectrally matched long duration and short duration set each containing 20 records. Since the short duration motions are spectrally matched to long-duration motions, the differences in the seismic response of the isolated bridges could be attributed to the difference in their duration characteristics.

Figure 1A compares the response spectrum of a long duration ground motion (from the 1992 Landers earthquake) and the spectrally equivalent short duration motion (from the 1986 Taiwan earthquake). Figure 1B shows the acceleration time histories of the two records. The list of selected 40 ground motions (20 long duration and 20 spectrally equivalent short duration motions) are provided in Table 1. Figure 2 shows the selected scaled short and long duration individual records along with their means as compared to the target spectrum.

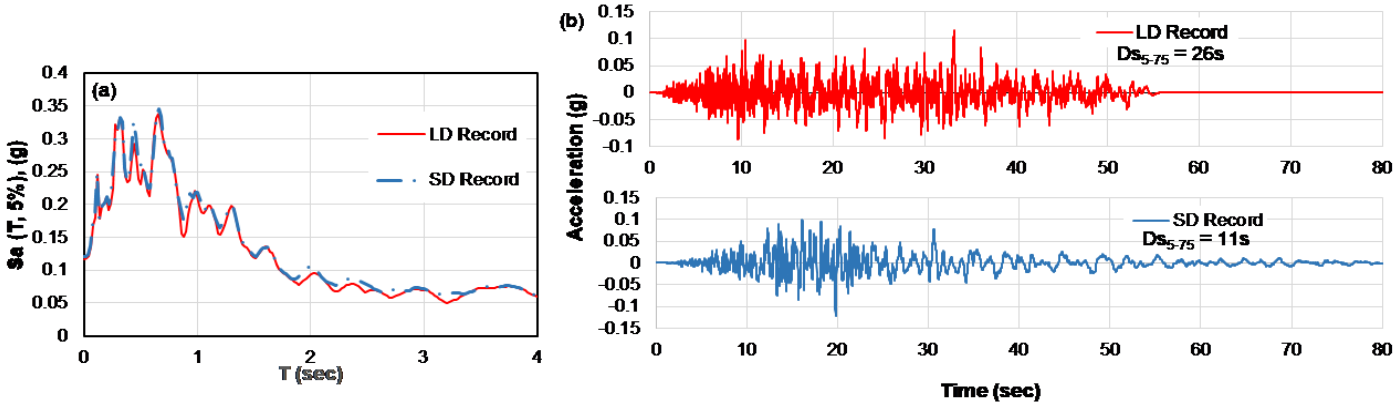

Figure1. Comparison of the (a) response spectra and (b) time histories of a spectrally equivalent long-duration and short-duration record (GM#1). The long-duration record is from the 1992 Landers earthquake, recorded at the Thousands palm post office station. The short-duration record is from the 1986 Taiwan earthquake, recorded at the SMART1 I11 station, scaled by a factor of 0.75.

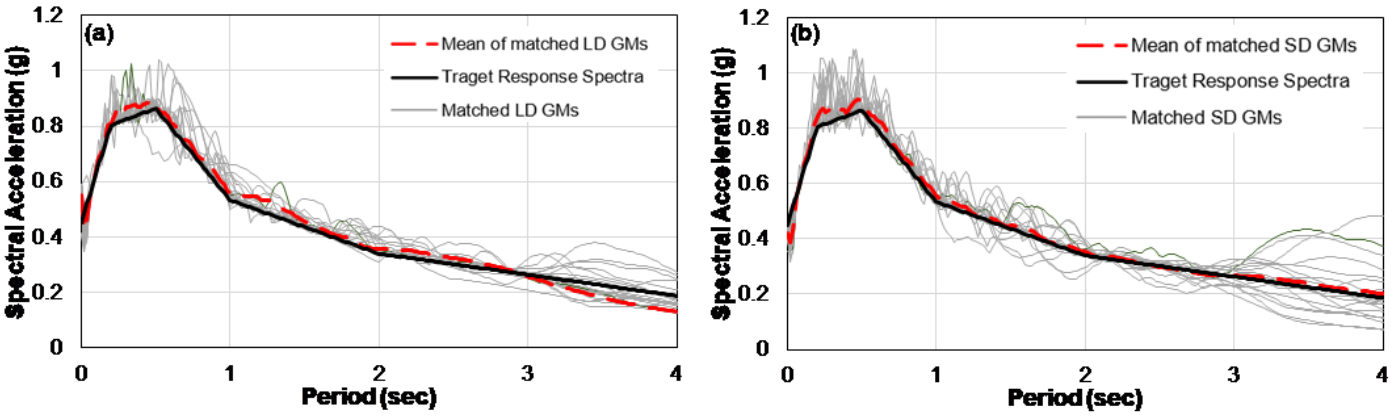

Figure 2. Mean response spectra for long-duration (a) and short-duration (b) ground motions compared to the target response spectrum of bridge location.

4 FINITE ELEMENT MODELING

A detailed three dimensional (3D) finite element model of the bridge is developed using a nonlinear fiber-based finite element program Seismostruct (Seismosoft 2020). The concrete superstructure, deck and girder, is modeled using an elastic beam element having equivalent stiffness and mass. Using the NU2000 girder geometry and concrete properties, the elastic beam elements are defined by calculating the values of EA, EI2, EI3 and GJ, where A is the cross-section area, E is the elastic modulus, I2 and I3 are the moments of inertia around local axes (2) and (3), G is the shear modulus, and J is the torsional constant. Based on the tributary area of each girder segment, lumped masses are defined on each girder. The circular concrete columns and the bent caps are modeled using forced-based fiber elements in Seismostruct. The confined and unconfined concrete and the steel materials constitutive relationship is defend following the hysteresis rule proposed by Mander et al. (1988) and Menegotto-Pinto stress-strain relationship (1973), respectively. However, to predict the actual effect of ground motion type, capturing the cyclic deterioration of the structure is crucial. Analytical

validation of experimental cyclic deterioration by Billah et al. (2017) demonstrates the accuracy of the program Seismostruct in predicting the cyclic strength degradation of structures under long duration motions.

Table 1. Database of long duration and spectrally equivalent short duration motion.

	Long Duration Motions					Spectrally matched short duration motion				
GM Pair No.	Earthquake	Year	Station	Magnitude	Ds 5-75 (s)	Earthquake	Year	Station	Magnitude	Ds 5-75 (s)
1	Landers	1992	Thousands Palm post office	7.2	26	Taiwan SMART1(45)	1986	SMART1 I11	6.3	11
2	Landers	1992	Indio-Jackson Road	7.2	26	Northridge-01	1994	Camarillo	6.7	14
3	Valparaiso, Chile	1985	Vina del Mar	7.8	32	Iwate	2008	Miyagino-ku	6.9	6
4	Valparaiso, Chile	1986	Zaplar	7.8	30	Morgan Hill	1984	Hollister Diff Array #1	6.2	11
5	Valparaiso, Chile	1985	Llolleo	7.8	28	Northridge-01	1994	Sun Valley - Roscoe Blvd	6.7	6
6	Valparaiso, Chile	1986	San Isidro	7.8	30	Christchurch, New Zealand	2011	SWNC	6.1	2
7	Maule, Chile	2010	Santiago Maipu	8.8	33	Northridge-01	1994	LA - Pico &Sentous	6.7	9
8	Maule, Chile	2010	Talca	8.8	53	Taiwan SMART1(5)	1986	SMART1 M10	6.3	4
9	Maule, Chile	20101	Angol	8.8	31	Irpinia, Italy-01	1980	Brienza	6.9	4
10	Tohuku, Japan	2011	Sendai	9.0	55	Kobe, Japan	1995	Kobe University	6.9	3
11	Tohuku, Japan	2012	Sakura	9.0	29	Chi-Chi, Taiwan-03	1999	CHY028	6.2	6
12	Tohuku, Japan	2011	Shiogama	9.0	56	Northridge-01	1994	Tarzana - Cedar Hill A	6.7	4
13	Tohuku, Japan	2012	Tsukidate	9.0	58	Iwate	2008	Maekawa Miyagi Kawasaki City	6.9	7
14	Michoacan, Mexico	1985	Villita Corona Centro	8.0	32	Darfield, New Zealand	2010	Heathcote Valley Primary School	7.3	8
15	Kocaeli, Turkey	1999	Fatih	7.5	28	Chi-Chi, Taiwan-06	1999	HWA025	6.2	3
16	Kocaeli, Turkey	2000	Bursa Tofas	7.5	26	Chi-Chi, Taiwan-04	1999	KAU085	6.2	20
17	El Mayor-Cucapah	2010	Ejido Saltillo	7.2	33	Chi-Chi, Taiwan	1999	TCU075	6.2	18
18	El Mayor-Cucapah	2010	Tamaulipas	7.2	27	Landers	1992	Amboy	7.2	17
19	Hokkaido, Japan	2003	Hayakita	8.3	25	Chi-Chi, Taiwan	1999	TTN026	6.2	20
20	ChiChi, Taiwan	1999	CHY008	7.6	32	Christchurch, New Zealand	2011	LINC	6.2	7

Since the bridge is supported on seat type abutments, the abutment response in both longitudinal and transverse directions is represented using bilinear springs as recommended by Caltrans and CHBDC. The gap between the deck and abutment is modeled using a zero-length nonlinear spring (bilinear gap element) following the suggestion of Muthukumar and Des Roches (2006). In this study, the isolation bearings are modeled using a zero-length link element. The hysteretic behavior of LRB is represented using a bilinear kinematic hardening model available in Seismostruct. Three parameters are needed to define the hysteresis behavior of LRB such as, the initial stiffness (Ki), post-yield hardening ratio (r), and yield force (Fy), which are obtained from the properties of LRB as shown in Table 3. For representing the SLRB, the zero-length bearing 1 element is used. Previously, Dezfuli and Alam (2018) showed that the bilinear kinematic hardening model could not accurately capture the response of SLRB under reversed cyclic loading. This bearing 1 element requires defining some dimensionless parameters A, β, and γ. The parameters β and γ represent the hysteretic shape variable

that controls the shape of the hysteretic loop. As suggested by Constantinou and Adnane (1987), the rule $A/(\beta+\gamma) =1$ is followed for defining the hysteretic shape variables. Following this, the values for the parameters A, β, and γ are defined as 1, 0.5, and 0.5, respectively.

Table 2. Properties of the three isolation bearings.

LRB			SLRB		
Parameter	Value	Unit	Parameter	Value	Unit
Characteristic Strength	187	kN	Shear Stiffness, Ks	9.3	kN/mm
Post Elastic Stiffness	1.75	kN/mm	SMA wire diameter	2.5	mm
Effective Stiffness	3.6	kN/mm	Superelastic strain limit	13.5	%
Yield Force	231	kN	Characteristic Strength	61	kN
Post-yield hardening ratio, r	0.19		Bearing hardening ratio	0.117	
Initial Stiffness, Ki	9.23	kN/mm			

5 RESULTS AND DISCUSSIONS

The seismic performance of the bridge isolated with LRB and SLRB isolation bearing under the LD and spectrally equivalent SD motions are compared in terms of different structural response parameters such as peak normalized base shear (PNBS),maximum isolator displacement (MID), residual isolator displacement (RID), in column, maximum pier deformation (MPD), and maximum deck acceleration (MDA). The seismic response of the isolated bridges subjected to the ground motions described above is compared through nonlinear time history analysis.

5.1 *Pier Base Shear*

In this study, the pier base shear in different isolated bridges under the two sets of ground motions is compared in terms of the peak normalized base shear (PNBS). The base shear obtained from the time history analysis of the different isolated bridges is normalized by the weight of the deck. Figure 3 compares the PNBS of the two isolated bridges under LD and SD motions. Figure 3a compares the response of LRB isolated bridge and Figure 3b shows the performance of SLRB isolated bridge. From Figure 3, it can be observed that irrespective of the isolation system used, the LD ground motions tend to increase the base shear demand in the pier. This can be attributed to the higher seismic energy imparted by LD motions which resulted in higher base shear demand. This outcome is in agreement with previous research, which has shown that LD motions increase the base shear demand. The largest individual PNBS is observed in the SLRB system under LD ground motions. Under the SD motions, the PNBS obtained from both isolation bearings are comparable and below 0.3. Under LD motions, SLRB experienced an average PNBS of 0.43 which is 0.34 for the LRB isolated system. The PNBS experienced under the LD motions is significantly larger for all three isolation systems as com-pared to the SD counterpart. This clearly indicates that the isolated bridges designed following current de-sign codes can significantly underestimate the substructure design forces under the LD ground motions.

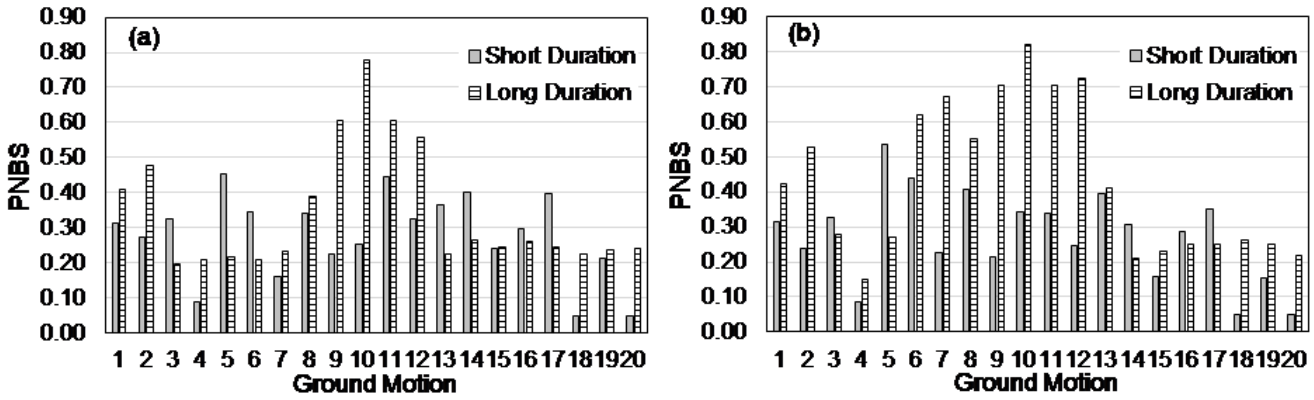

Figure 3. Peak normalized base shear (PNBS) for bridge piers isolated with different isolation bearings under LD and SD ground motions (a) LRB and (b) SLRB.

5.2 *Maximum Pier Displacement*

Maximum pier top displacements of the bridges isolated with LRB and SLRB are compared in Figure 4. Isolation bearings are known to increase peak displacement responses of the isolated piers, which is a direct consequence of increasing the lateral flexibility resulting from the isolation bearings. The effect of LD motions is clearly reflected in Figure 4. Irrespective of the isolation bearing used, LD motions imparted higher displacement demand on the bridges as observed from increasing pier top displacement. Large number of displacement reversals resulted in higher damage under the LD motions that subsequently increased the pier flexibility and thereby increased the maximum pier displacement. The LRB isolated bridge pier experienced maximum average displacement of 53mm which is 20% higher than the SLRB isolated bridge pier average maximum displacement under the LD motions. On the other hand, under the SD motions, SLRB isolated pier experienced the smallest deformation which is 25% less than the LRB system. Evaluation of the pier top displacement for all three isolation systems reveals that there is an average 30% increase in MPD under the LD motions as compared to the SD motions.

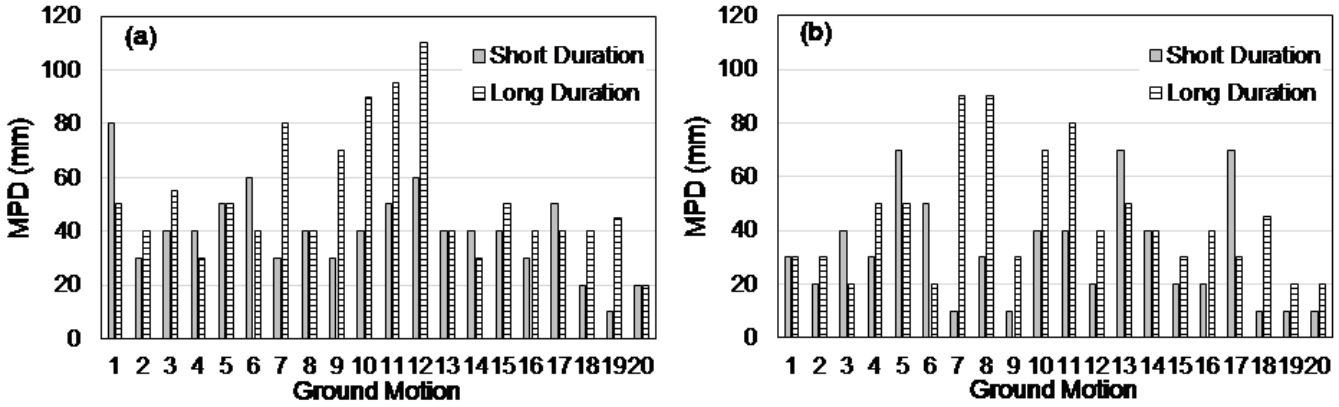

Figure 4. Maximum pier displacement (MPD) for bridge piers isolated with different isolation bearings under LD and SD ground motions (a) LRB and (b) SLRB.

5.3 *Maximum Deck Acceleration*

The acceleration of the bridge deck is proportional to the earthquake's forces exerted to the structure. The main responsibility of the isolation system is to significantly reduce the deck acceleration by isolating the superstructure from the substructure. Figure 5 compares the deck acceleration in the isolated bridges under the LD and SD ground motions. Both bridge systems experienced higher deck accelerations when subjected to LD ground motions. From the results presented in Figure 5, it can be observed that SLRB effectively reduced the bridge deck acceleration as compared to the LRB system irrespective of the ground motion duration. Although SLRB resulted in higher shear force in the pier but resulted in smaller deck acceleration. Dezfuli and Alam [40] reported a similar observation where they compared the performance of SLRB and LRB under near-fault ground motions. For the LRB system, the LD motion increased the deck acceleration by 30% as compared to the SD motions whereas this increase is 25% for the SLRB system.

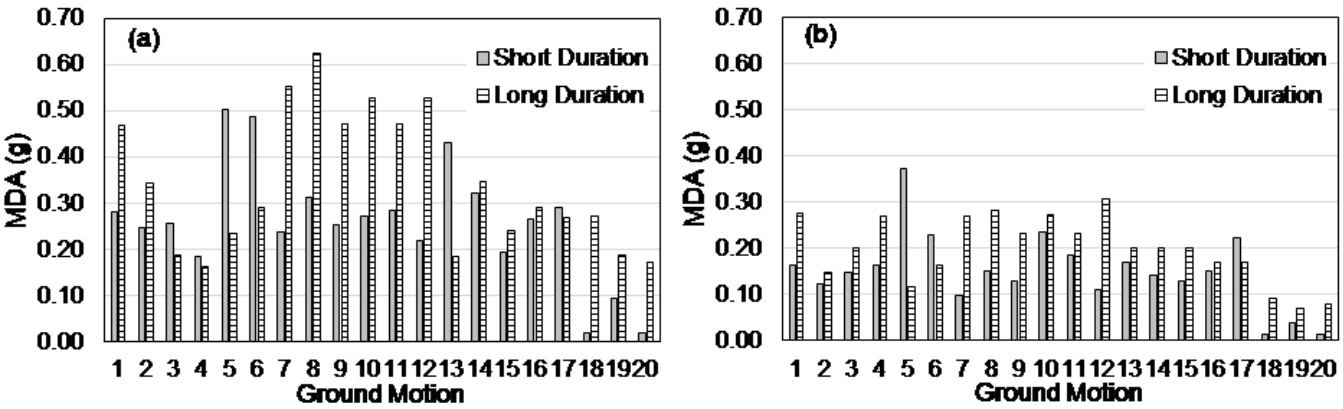

Figure5.Maximum deck acceleration (MDA) for bridge piers isolated with different isolation bearings under LD and SD ground motions (a) LRB and (b) SLRB.

5.4 *Isolation Bearing Response*

The performance of the two isolation bearings is compared in terms of maximum isolator displacement (MID) and residual isolator displacement (RID) obtained from the nonlinear time history analyses using 40 ground motions. Figure 6 compares the LRB and SLRB MID response under the LD and SD motions. The LRB experienced larger MID as compared to SLRB irrespective of the ground motion type. As seen from Figure 6, the SD motions tend to impose higher deformation on the isolation bearings as compared to the LD motions irrespective of the bearing types. For example, the SD motion increases the MID for LRB on an average by 20% whereas it is increased by 35% for SLRB. Among the two bearings, SLRB sustained the smallest MID for both SD and LD ground motions.

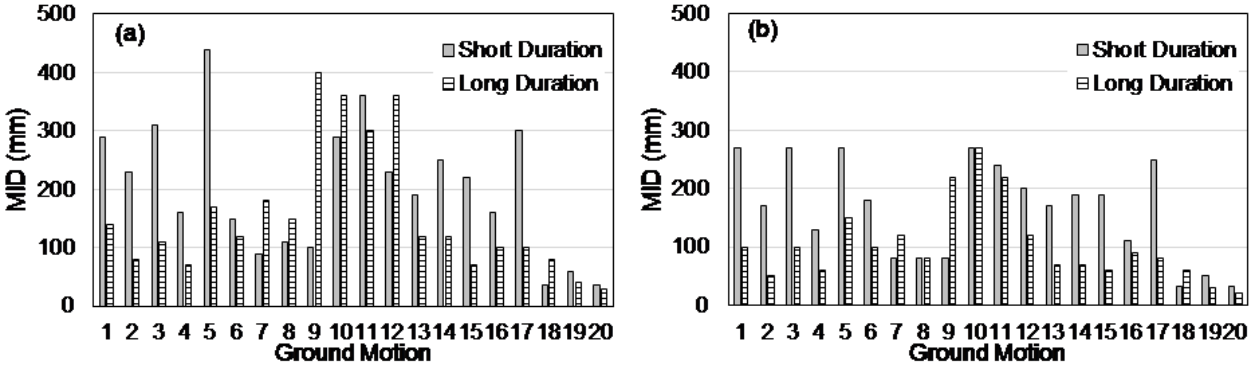

Figure 6. Maximum isolator displacement (MID) for bridge piers isolated with different isolation bearings under LD and SD ground motions (a) LRB and (b) SLRB.

The post-earthquake functionality of bridges is one of the major requirements of the current performance-based seismic design. Isolation bearings need to have an adequate re-centering capacity to ensure the post-earthquake functionality of bridges. A large amount of residual deformation, accumulated after the end of an earthquake, indicates the inadequate restoring capacity of the isolation system [60]. Different researchers proposed several advanced isolation systems for controlling the residual displacement in isolation bearings [38, 39, 61, 62]. Figure 7 shows the comparison of residual isolator displacement (RID) experienced by different isolations systems under the LD and SD motions. From Figure 7, it is evident that irrespective of the bearing used, the LD motions tend to increase the RID significantly. The results show that the SLRB system is successful in recovering the deformation at the end of ground motions for both LD and SD motions. Under the SD motions, SLRB experienced an average RID of 10mm, which is increased up to 14mm under the LD motions. The re-centering ability of the SMA wires used in the SLRB system resulted in the near-perfect restoring characteristics. On the other hand, the LRB system experienced 28mm RID under the SD motions, which is in-creased by more than two times under the LD motions.

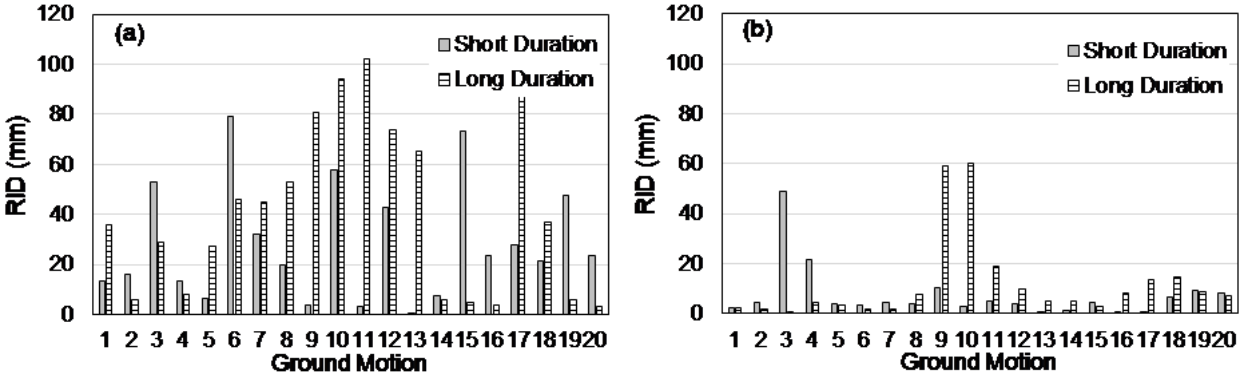

Figure 7. Residual isolator displacement (RID) for bridge piers isolated with different isolation bearings under LD and SD ground motions (a) LRB and (b) SLRB.

Figure 8 shows the relationship between the ground motion duration, magnitude, and the accumulated residual displacement in different isolation systems under long duration motions. From Figure 8 it can be seen that, as

the ground motion duration and magnitude increase, the RID also increases. However, a large magnitude does not affect the RID if the duration is smaller. For example, when the LRB is subjected to the Mw 8.8 motion with a significant duration of 31s (LD#9), the RID is 45mm. On the other hand, when the significant duration is increased to 53s under Mw 8.8 motion (LD#8), the RID is increased by 200% to 135mm. It is to be noted that both LD#8 and LD#9 are the recorded ground motions from the 2010 Maule, Chile earthquake recorded at different stations. This clearly indicates the ground motion duration significantly affects the restoring capacity of the isolation bearing which can significantly affect the post-earthquake functionality of the bridge.

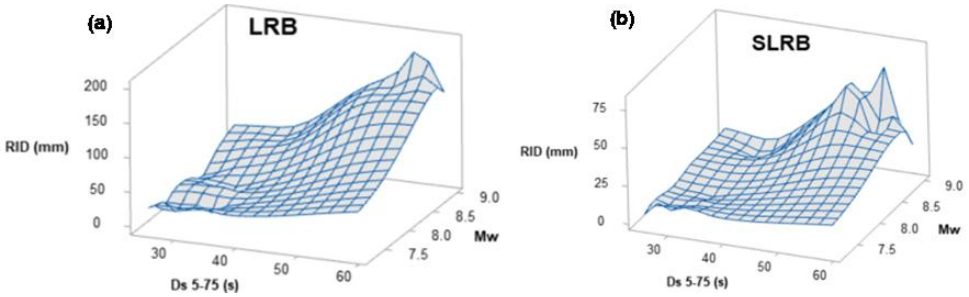

Figure 8. Relationship of residual isolator displacement (RID) with significant duration and magnitude under LD ground motion.

6 CONCLUSIONS

This paper assessed the seismic performance of LRB and SLRB isolated bridges in terms of pier displacement, shear force, deck acceleration, and isolator maximum and residual displacement considering variability in ground motion duration. Using nonlinear time history analyses, the effect of long duration motion on the response of seismically isolated bridges are evaluated. Based on the outcome of the numerical analysis, the following conclusions are drawn:

- Long duration motions cause more damage to different bridge components as compared to the short duration motions in-terms of higher deck acceleration, pier base shear, and residual isolator displacement.
- Under LD motions, isolated bridge piers are susceptible to significantly higher shear force as compared to SD motions.
- SLRB system is an effective option for reducing the isolator residual displacement and improving the post-earthquake functionality of bridges under LD motions.
- Testing requirements should be imposed to evaluate the damping mechanism and energy dissipation capacity under a large number of displacement reversals before implementing in sites susceptible to long-duration motions.

REFERENCES

Alam MS, Bhuiyan MAR, Billah AHMM. Seismic fragility assessment of SMA-bar restrained multi-span continuous highway bridge isolated by different laminated rubber bearings in mediumto strong seismic risk zones. Bull EarthqEng 2012; 10:1885–909.

Al-Anany Y, Moustafa MA, Tait M. Modeling and evaluation of a seismically isolated bridge using unbonded fiber-reinforced elastomeric isolators. Earthq Spectra 2018; 34(1):145–68.

Amin, A.F.M.S., Wiraguna, S.I., Bhuiyan, A.R., Okui, Y., 2006. Hyperelasticity model for FE analysis of natural and high damping rubbers in compression and shear. J. Eng. Mech., ASCE 132 (1), 1–11.

Ancheta TD, Darragh RB, Stewart JP, Seyhan E, Silva WJ, Chiou BSJ, Wooddell KE, Graves RW, Kottke AR, Boore DM, KishidaT, Donahue JL. PEER NGA-West2 Database, PEER 2013/03,PEER Center. Berkeley, California: University of California,2011.

Baker JW, Cornell CA. Spectral shape, epsilon and record selection. Earthq. Engr.Struct.Dyn. 2006; 35(9): 1077–1095.

Bhuiyan M A R and Alam M S 2013 Seismic performance assessment of highway bridges equipped with superelastic
shape memory alloy-based laminated rubber isolation bearing Eng. Struct. 49 396–407.

Billah AHMM, Todorov B. Effects of subfreezing temperature on the seismic response of lead rubber bearing isolated bridge. Soil Dynamics and Earthquake Engineering 2019;126.

Billah AHMM, Kabir MR, Alam MS. Comparative collapse performance assessment of bridge pier under near-fault and long-duration ground motions. 16th world conference on earthquake engineering, Santiago, Chile. January 2017.

Canadian Standard Association – CSA. CAN/CSA-S6-19: Canadian highway bridge design code. National Research Council of Canada, Ottawa; ON.

Chandramohan R, Baker JW, Deierlein GG. Quantifying the influence of ground motion duration on structural collapse capacity using spectrally equivalent records. Earthquake Spectra, 2016; 32(2): 927–950.
Center for Engineering Strong Motion Data (CESMD), 2012. Center for Engineering Strong Motion Data. [online] Available at: <http://www.strongmotioncenter.org/> [Accessed 1 June2019].
Constantinou MC, Adnane MA. Dynamics of Soil-Base-Isolated Structure Systems: Evaluation of Two Models for Yielding Systems. Report to the National Science Foundation 1987,Department of Civil Engineering, Drexel University, Philadelphia, PA.
Dicleli M. Performance of seismic-isolated bridges in relation to near-fault ground-motion and isolator characteristics. Earthquake Spectra 2006; 22(4):887–907.
Eröz M, DesRoches R. A Comparative Assessment of Sliding and Elastomeric Seismic Isolation in a Typical Multi-Span Bridge. Journal of Earthquake Engineering 2013; 17(5): 637-657.
Marafi NA, Eberhard MO, Berman JW, Wirth, EA, Frankel AD. Impacts of Simulated M9Cascadia Subduction Zone Motions on Idealized Systems. Earthquake Spectra 2019; 35(3) :1261-1287.
Mander JB, Priestley MJN, Park R. Theoretical stress-strain model for confined concrete. JStructEng ASCE 1988; 114(8):1804–26.
Menegotto M, Pinto PE. Method of analysis for cyclically loaded R.C. plane frames including changes in geometry and non-elastic behaviour of elements under combined normal force and bending. Symposium on the Resistance and Ultimate Deformability of Structures Acted on by Well Defined Repeated Loads. International Association for Bridge and Structural Engineering, Zurich, Switzerland, 1973; 15-22.
Muthukumar S, DesRoches R. A Hertz contact model with non-linear damping for pounding simulation. EarthqEngStructDyn 2006; 35:811–28.
Ozbulut OE, Hurlebaus S. Optimal design of superelastic-friction base isolators for seismic protection of highway bridges against near-field earthquakes. Earthquake Engineering and Structural Dynamics 2011; 40: 273–291.
Ozdemir G, Avsar O, Bahyan B. Change in response of bridges isolated with LRBs due to leadcore heating. Soil DynEarthqEng 2011; 31:921–9.
SeismoSoft. SeismoStruct - a computer program for static and dynamic nonlinear analysis offramed structures available from: www.seismosoft.com; 2020.
Shen J, Tsai MH, Chang KC, Lee GC. Performance of a Seismically Isolated Bridge under Near-Fault Earthquake Ground Motions. Journal of Structural Engineering 2004; 130(6): 861-868.
Tongaonkar NP, Jangid RS. Seismic response of isolated bridges with soil-structure interaction. Soil DynEarthqEng 2003; 23:287–302.
Warn GP and Whittaker AS. Performance estimates in seismically isolated bridge structures, Engineering Structures. 2004; 26: 1261–1278.